Lithuanian Journal of Physics
Vol. **64**, No. 1, pp. 11–19 (2024)
ISSN 1648-8504 eISSN 2424-3647
DOI: https://doi.org/10.3952/physics.2024.64.1.2

PREDICTING NONRADIATIVE DECAY BARRIER OF BODIPY DYE IN POLAR ENVIRONMENT BY APPLYING ONIOM MULTISCALE METHOD

D. Narkevičius and S. Toliautas

Faculty of Physics, Vilnius University, Saulėtekio 9, 10222 Vilnius, Lithuania
Email: domantas.narkevicius@ff.stud.vu.lt

Received 7 July 2023; accepted 18 August 2023

Fluorescent molecular sensors are widely used in biological research. They allow straightforward viscosity, temperature or polarity measurements at the microscopic level, including live cells. Maps of desired physical properties can be obtained by applying fluorescence lifetime imaging microscopy (FLIM) to cells.

One of the most important properties of a cell is viscosity, as it affects other parameters, such as the rate of biochemical reactions and particle diffusion. Boron-dipyrromethene (BODIPY) compounds are widely used for viscosity measurements, but current variants have the undesirable sensitivity to polarity, and more suitable alternatives are being sought using theoretical computations. The polarizable continuum model (PCM) used in previous studies did not adequately take into account the influence of the polar environment when calculating the BODIPY activation energy associated with polarity sensitivity.

After applying the multilayer ONIOM method in polar and non-polar environments, the calculated maximum wavelengths of the fluorescence spectra of the 8PhBODIPY compound were closer to the experimental results compared to PCM. The activation energy was also calculated, its value in polar and non-polar environments qualitatively corresponded to the experimental results, and the quantitative agreement was reached using the empirical correction.

Keywords: fluorescent probes, molecular rotors, BODIPY, DFT, ONIOM

1. Introduction

Fluorescent molecular sensors are widely used in current biological research [1]. They allow a convenient measuring of various physical properties (viscosity [2–4], temperature [5, 6], and polarity [7, 8]) in a medium. The primary reason for using such probes is their ability to measure on a microscopic scale, where conventional methods are impossible, e.g. in cells. By applying fluorescence lifetime imaging microscopy (FLIM), maps of the desired physical property of living cells can be obtained [9–11].

One of the cell characteristics is viscosity, which determines the rate of biochemical reactions, diffusion, and physical properties. There is evidence that cell viscosity changes with the development of certain diseases [12]. Thus, it is essential to develop viscosity probes with desired properties. A subset of fluorescent compounds – molecular rotors – have sensitivity to this physical quantity because the molecule contains a rotating part the movement of which is restricted by the friction (viscosity) of the surrounding medium [13, 14]. The rotation is also constrained by the steric hindrance of the molecule, which creates an energy barrier between two existing conformers of the molecule. Due to the presence of thermal energy at non-zero temperature the molecule can cross this energy barrier, so each viscosity sensor is also a temperature sensor. Boron-dipyrromethene (BODIPY) viscosity sensors are widely used [15] because their fluorescence kinetics are often single-exponential, which speeds up the interpretation of experiments. Despite their advantages, BODIPY probes have a few drawbacks. Upon the polarity change of the medium, the measured photophysical properties of BODIPY compounds also change. Thus only by knowing the exact polarity properties of a system, the measured results can be interpreted unambiguously.

When designing a BODIPY molecule, theoretical computations are essential for predicting physical properties in various environments. There is an interest in a proper model for simulating molecules, similar to the one established for BODIPY compounds in non-polar solvents, which utilizes the polarizable continuum model (PCM) [16]. Potential energy surface (PES) scans of BODIPY with PCM cannot predict quantitative or even qualitative properties of conformational transition barriers in the polar environment, as they yield higher energy of the barrier compared to the non-polar medium, which is contrary to the results of current research [12]. The basic idea of why PCM does not work with the polar environment is that solvent molecules with dipole moments interact in a specific way with excited BODIPY molecules, and PCM, by definition, cannot model such interactions. Therefore, an explicit solvation method incorporating distinct solvent molecules is needed.

2. Theoretical and experimental methods

Most commonly, density functional theory (DFT) [17, 18] is used for quantum-chemical modelling of BODIPY dyes because it offers an excellent accuracy compared to the computational cost. However, its usage is still limited to the closest solvent molecules around the fluorescent BODIPY compound. For modelling larger systems, a multiscale ONIOM [19] model can be employed, which allows the system to be treated using multiple levels of computational theory.

Preliminary testing found that simply placing solvent molecules around the BODIPY dye created localized areas with excess solvent molecules, which produced localized charges, and the results of calculated fluorescence were all over the place with the increasing number of solvent molecules. For this reason, the preparation of the solvent shell was carried out using molecular dynamics (MD). The symmetric solvent sphere was constructed by the following procedure:

1. A single molecule of the desired solvent is created using *AmberTools21* [20].

2. Single-molecule geometry is optimized at the molecular mechanics (MM) level theory with a *gaff2* force field. The same force field is used for all subsequent steps.

3. The optimized solvent molecule is placed n times at a given radius r using *Packmol* [21], creating the initial solvent sphere. Ultimately, two different sphere radii (corresponding to a specific quantity of molecules denoted as n) were chosen for each modelled solvent (Table 1).

Table 1. The initial number of solvent molecules for the selected sphere radii.

	r_1 = 15 Å	r_2 = 19 Å
C_5H_{12}	50	100
CH_3CN	110	220

4. The total potential energy of the entire solvent system is minimized.

5. The thermal annealing procedure is carried out. First, the sphere is rapidly heated up to 50 K, which corresponds to the temperature at which molecules can mix but cannot dissociate into a vacuum. Afterwards, a slow cooling is performed every 10 K to ~0 K. The system is held for 100 ps at the corresponding temperature during each step.

6. The final energy minimization is performed.

After creating a symmetric solvent sphere, the 8-Ph-BODIPY dye (Fig. 1) is inserted in the centre, and the solvent molecules that intersect the molecule are removed. Thus, the total count of solvent molecules is fewer than that in Table 1. Also, after the MD procedure, the modelled sphere takes an ellipsoid-like form. During the dye insertion, the molecule rotation is then aligned with

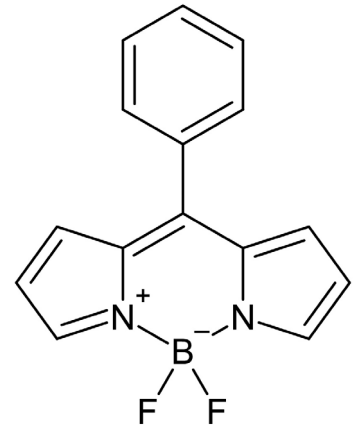

Fig. 1. The molecular structure of the 8-Ph-BODIPY compound.

the direction of the ellipsoid, preventing any asymmetries from occurring. An example of the solute–solvent system is shown in Fig. 2.

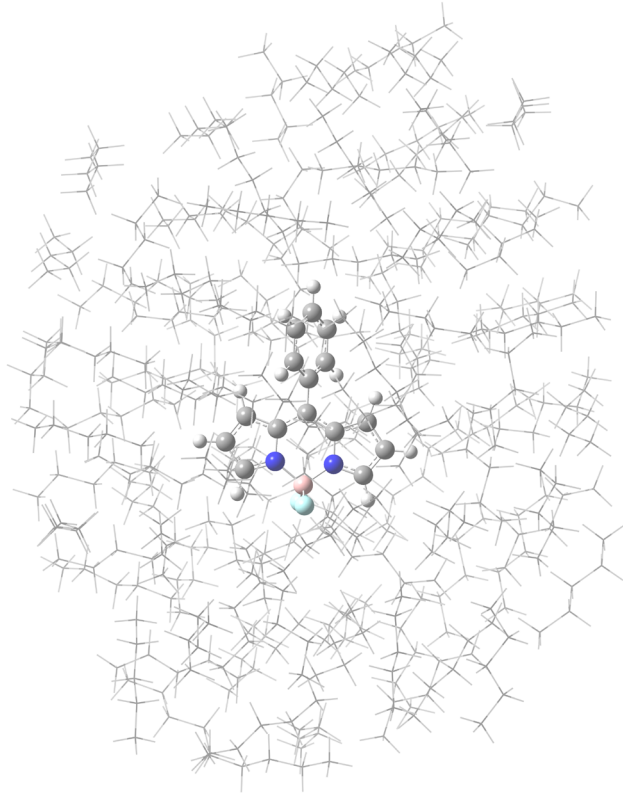

Fig. 2. An example of the BODIPY compound position in the pentane solvent ellipsoid.

After the preparation of the system, its potential energy was optimized to the ground state using a Minnesota density functional *m06-2x* [22, 23] with a *cc-pVDZ* [24] basis set for the 8-Ph-BODIPY molecule, while solvent molecules were modelled with MM using a universal force field (UFF) [25]. For the case of implicit solvation, a conductor-like PCM [26] was employed instead of explicit solvent molecules. For QM and QM/MM calculations, Gaussian 16 software was used [27]. After that, optimization of the molecular structure to find the energy minimum of the first excited state was performed, which then resulted in a value of the theoretical fluorescence wavelength. Overall, BODIPY has a multireference wavefunction character, thus transition energies are overestimated [23]. Despite this drawback, the overestimation is systematic. Therefore, if needed, an empirical calibration could be performed [28]. For the analysis of ONIOM results presented here, only DFT-layer energy was considered.

After finding the optimized excited-state geometry, a relaxed scan is performed, where the scanning coordinate is one of the dihedral angles between the phenyl plane and the BODIPY core [29] (φ_1, Fig. 3). After that, the average (Θ) of dihedral angles (φ_1 and φ_2, Fig. 3) between two BODIPY sides is calculated, which is the approximate intrinsic coordinate. From the scan, we get three points of interest: S_1 metastable (S_{1m}), relaxed (S_{1r}) and transitional states (TS). By calculating the height of the barrier (which may occur between the scan points) using the *Akima* interpolator [30] with Savitzsky–Golay filtering and choosing S_{1m} energy as a zero point, activation energy will be equal to transition energy.

Toluene (Tol) and dimethylformamide (DMF) were chosen for the implicit solvation. The reasoning is that both solvents are aprotic, meaning that hydrogen bonds do not play a role in calculations, simplifying the model. Acetonitrile (MeCN) and pentane (C_5H_{12}) were chosen for the explicit solvation. These solvents are very similar to DMF and Tol, respectively, regarding their dielectric constants, which allows for comparison of the trends

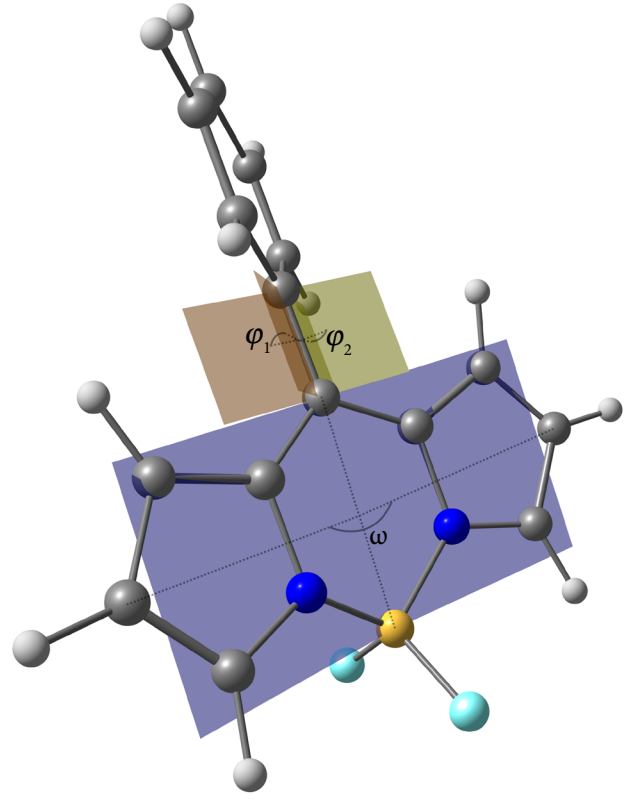

Fig. 3. Dihedral angles of 8-Ph-BODIPY used for PES scans and geometry comparison.

of the barrier height between polar and non-polar environments. Also, MeCN is one of the smallest non-protic molecules, allowing a simpler re-arrangement of molecules around the 8-Ph-BODIPY dye, while C_5H_{12} is one of the smallest non-aromatic non-polar solvents. Aromaticity can induce the π–π stacking effect with the fluorophore, which again would introduce further complications to the model.

Experimental studies were performed on the pre-synthesized 8-Ph-BODIPY. First, the solid dye was dissolved in toluene at a concentration of 4 mM. Then, 2 μL of the initial solution was diluted to 2 mL with the desired solvent, and the final solution was poured into a quartz 1 cm cuvette. The final concentration was 4 μM.

An Edinburgh Instruments FL920 fluorometer based on single photon counting was used for fluorescence measurements. A 472.7 nm pulsed laser with a period of 500 ps was used for the excitation. Fluorescence spectra were measured at the maximum laser power, with photons collected every 0.5 nm for 2 s, from 495 to 700 nm, with a wavelength bandwidth of 2 nm. Before exciting the sample, the laser beam was passed through an SP550 filtre, and the fluorescence beam went through an LP495 slide.

3. Results and discussion

The maximum wavelengths of the experimental 8-Ph-BODIPY spectra are provided in Table 2. There is some solvatochromism for absorption: in the measured data, the absorption wavelength is the lowest for acetonitrile, then pentane and toluene. Fluorescence in acetonitrile and pentane has the same peak wavelength, even though their polarity is very different. Toluene has the lowest fluorescence energy. The reasoning behind these results is that toluene, an aromatic solvent, interacts with 8-Ph-BODIPY via the π–π stacking effect. Thus, the overall π system extends, and the resulting transition energy is lower for both absorption and fluorescence. Having the same fluorescence wavelength in the pentane and acetonitrile may be due to a weak charge transfer in the BODIPY molecule after the initial excitation.

The calculated transition energies from S_0 to S_1 are found in Table 3. All energies are relative to the S_0 minimum in the corresponding environment. E_1 is the energy of the optimised excited state, while E_0 is the ground state energy of the excited state geometry. In the PCM-modelled non-polar environment, toluene and pentane have the same wavelength, which is opposite to the experimental results. It is now evident that PCM cannot consider the π–π interaction effect. Also, there is a considerable transition energy decrease going from the non-polar into the polar environment in PCM, while the experiment again shows different results. Looking at the ONIOM-modelled fluorescence, the wavelength is still higher in the polar environment, but the wavelengths are much closer compared to pentane, just like in the experiment. Even though the absolute difference to the experiment in ONIOM is higher than using PCM (also, ONIOM has higher energies of E_0 and E_1), ONIOM can model fluorescence transition energies better than PCM after considering corrections.

Table 2. Experimental maxima of 8-Ph-BODIPY fluorescence and absorption spectra.

Solvent	λ_{fl}, nm	λ_{abs}, nm	ε_r
n-Pentane	515	499	1.8
Toluene	522	503	2.4
Acetonitrile	515	496	36.6

The calculated geometries with PCM and the explicit solvation method are summarized in Table 4. For the ground state, higher core bending ω in the polar environment is present compared to the non-polar environment in both solvation methods. Phenyl rotation in S_0 is very similar except for the case with a thicker MeCN sphere, which is about ten degrees lower than the rest. Looking at the geometries in S_1, core bending is much higher in vacuum or toluene. In pentane, the core almost does not change the geometry compared to the ground state. There is a rough correlation between geometry and the transition energies: by folding the BODIPY core more in an excited state compared to the ground state, we get lower transition energy, and by restricting the folding, we get lower wavelength fluorescence. The explicit solvation model puts a higher force on the BODIPY molecule when transitioning between energy levels.

In Fig. 4, the PES relaxed scans of 8-Ph-BODIPY molecule are plotted in different environments. While performing the PES scans with explicit

Table 3. Calculated potential energy values of 8-Ph-BODIPY. E_0 and E_1 are the energies of S_0 and S_1 surfaces at the optimized S_{1m} geometry. Energy values are relative to the S_0 minimum in the corresponding environment.

Environment	Solvation	E_0, eV	E_1, eV	ΔE, eV	λ, nm	ε_r
Vacuum	–	0.125	3.016	2.89	429	1
n-Pentane	PCM	0.045	2.815	2.77	448	1.8
Toluene		0.078	2.844	2.77	448	2.4
Acetonitrile		0.047	2.685	2.64	470	36.6
DMF		0.056	2.681	2.63	472	38.3
C_5H_{12} ×48	ONIOM	0.063	3.047	2.98	415	–
C_5H_{12} ×97		0.065	3.039	2.97	417	–
CH_3CN ×106		0.078	3.023	2.95	421	–
CH_3CN ×216		0.110	3.012	2.90	427	–

Table 4. Dihedral angles of the optimized 8-Ph-BODIPY in different environments and electronic energy states.

Environment	S_0		S_{1m}	
	Θ, °	ω, °	Θ, °	ω, °
Vacuum	54	174	45	161
Toluene	53	179	46	166
C_5H_{12} ×48	56	179	52	179
C_5H_{12} ×97	53	178	52	179
DMF	52	176	48	169
MeCN ×106	50	174	45	170
MeCN ×216	43	174	37	172

solvation, there were encounters when a significant solvent reorientation was detected, which resulted in a jump in system energy. This observation was mainly in lower-radius solvent spheres, which suggests an insufficient number of solvent molecules. When a drop in energy was observed, an additional reverse scan was performed, often resulting in lower PES curves. The lowest points with a reasonable curve path were ultimately taken for interpolation and smoothing.

The minima at S_{1r} are supposed to be at 0 degrees because of the C_s symmetry of the molecule. Using the smaller solvent sphere, the minima are at ~7.5° for both polar and non-polar solvents,

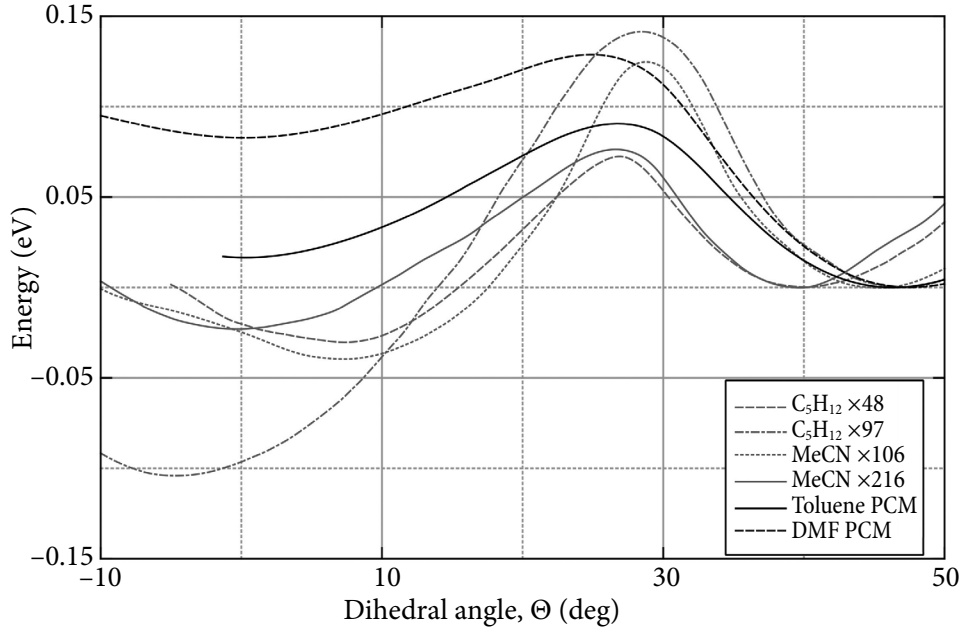

Fig. 4. Relaxed PES scans of 8-Ph-BODIPY in different solvent environments.

while in a larger sphere, in the polar environment it is ~0° and in the non-polar case it is equal to –4.7°, which is closer to 0°. Considering the significant reorientation of solvent molecules and the fact that S_{1r} minima are not at 0° for smaller spheres, modelling 8-Ph-BODIPY in a larger sphere can be stated to give more accurate results, and only those were used when comparing performance with PCM.

Interestingly, even though the energy minimum of the DFT layer in a larger non-polar solvent sphere does not lie at 0°, the total ONIOM energy does. That means that fluorophore creates a significant asymmetric interaction with the solvent molecule. Doing population analysis on the whole system (semi-empirical PM6 method [31]), one side of the phenyl ring has a higher wavefunction overlap (Fig. 5) with the solvent at the highest occupied molecular orbital (HOMO). In contrast, in the polar environment this effect is not seen. The possible reason for such supermolecular effect is that solvent spheres used are still not large enough. Furthermore, this might be a reason behind a rough correlation between the S_{1r} minimum position and the *r* radius.

Table 5 shows the activation energy of fluorophore from different states and the energy change (enthalpy). At first glance, enthalpy in PCM is positive, while in ONIOM it is negative in all cases. Compared with higher-level calculations [32], ONIOM gives qualitatively correct results, while PCM does not. PCM quantitatively predicts the activation energy (going from S_{1m} through TS) in a non-polar solvent very well (the experimental

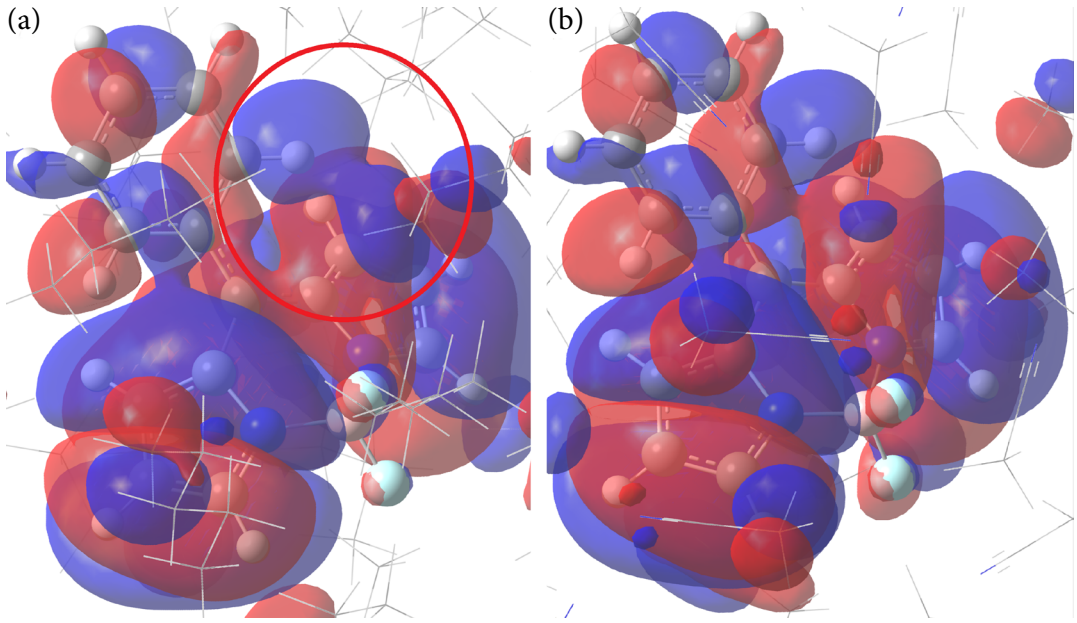

Fig. 5. HOMO orbital for 8-Ph-BODIPY in the C_5H_{12} ×97 (a) and the CH_3CN ×217 (b) solvent shell. Isovalue is at 0.0015. The overlap between the solvent molecule and 8-Ph-BODIPY is circled in red.

Table 5. Enthalpy change going from S_{1m} to S_{1r} and the activation energies of 8-Ph-BODIPY.

Environment	$\Delta H(S_{1r}–S_{1m})$, eV	$E_a(TS–S_{1r})$, eV	$E_a(TS–S_{1m})$, eV
Tol PCM	0.016	0.074	0.091
C_5H_{12} ×48	–0.030	0.103	0.072
C_5H_{12} ×97	–0.104	0.246	0.141
DMF PCM	0.083	0.046	0.129
MeCN ×106	–0.040	0.164	0.125
MeCN ×216	–0.023	0.099	0.076

value is 0.103 eV [16]). However, in the polar environment it does not even reproduce results qualitatively: the barrier in DMF is higher than in toluene, while in the polar environment it is measured to be about 0.032 eV [16]. On the other hand, the barrier in a larger sphere calculated with the ONIOM method is higher in the non-polar environment and much lower in the polar one. A simple correction by subtracting 0.04 eV from the calculated values would even produce values comparable to the experiment.

4. Conclusions

The explicit solvation with the ONIOM model improved the modelling results of 8-Ph-BODIPY optical properties in several areas. The calculated fluorescence wavelengths in different environments were much closer to each other (and in agreement with the experiment) compared to the PCM implicit solvation method. S_{1r} (relaxed) and S_{1m} (metastable state) energy levels calculated with ONIOM were closer to the higher-level calculation results reported elsewhere. Also, the explicit solvation reproduced qualitative changes of the excited state barrier height in different environments (inferred from experiments), where PCM previously failed.

Even with these improvements, calculating the PES in the solvent shell using ONIOM was difficult because of solvent reorientation. This problem may be addressed using the rigid PES, a larger solvent sphere or additional system preparation using molecular dynamics together with the fluorophore.

Acknowledgements

Computations were performed using resources at the supercomputer 'VU HPC' of Vilnius University at the premises of the Faculty of Physics.

References

[1] K. Maleckaitė, D. Narkevičius, R. Žilėnaitė, J. Dodonova-Vaitkūnienė, S. Toliautas, S. Tumkevičius, and A. Vyšniauskas, Give or take: effects of electron-accepting/-withdrawing groups in red-fluorescent BODIPY molecular rotors, Molecules **27**(1), 23 (2021), https://doi.org/10.3390/molecules27010023

[2] M. Kubánková, I. López-Duarte, D. Kiryushko, and M.K. Kuimova, Molecular rotors report on changes in live cell plasma membrane microviscosity upon interaction with beta-amyloid aggregates, Soft Matter **14**(46), 9466–9474 (2018), https://doi.org/10.1039/C8SM01633J

[3] J.E. Chambers, M. Kubánková, R.G. Huber, I. López-Duarte, E. Avezov, P.J. Bond, S.J. Marciniak, and M.K. Kuimova, An optical technique for mapping microviscosity dynamics in cellular organelles, ACS Nano **12**(5), 4398–4407 (2018), https://doi.org/10.1021/acsnano.8b00177

[4] H. Xiao, P. Li, and B. Tang, Small molecular fluorescent probes for imaging of viscosity in living biosystems, Chem. Eur. J. **27**(23), 6880–6898 (2021), https://doi.org/10.1002/chem.202004888

[5] M. Homma, Y. Takei, A. Murata, T. Inoue, and S. Takeoka, A ratiometric fluorescent molecular probe for visualization of mitochondrial temperature in living cells, Chem. Commun. **51**(28), 6194–6197 (2015), https://doi.org/10.1039/C4CC10349A

[6] M.M. Ogle, A.D. Smith McWilliams, B. Jiang, and A.A. Martí, Latest trends in temperature sensing by molecular probes, ChemPhotoChem **4**(4), 255–270 (2020), https://doi.org/10.1002/cptc.201900255

[7] H. Sunahara, Y. Urano, H. Kojima, and T. Nagano, Design and synthesis of a library of BODIPY-based environmental polarity sensors utilizing photoinduced electron-transfer-controlled fluorescence ON/OFF switching, J. Am. Chem. Soc. **129**(17), 5597–5604 (2007), https://doi.org/10.1021/ja068551y

[8] H. Xiao, P. Li, and B. Tang, Recent progresses in fluorescent probes for detection of polarity, Coord. Chem. Rev. **427**, 213582 (2021), https://doi.org/10.1016/j.ccr.2020.213582

[9] D. Jurgutis, G. Jarockyte, V. Poderys, J. Dodonova-Vaitkuniene, S. Tumkevicius, A. Vysniauskas, R. Rotomskis, and V. Karabanovas, Exploring BODIPY-based sensor for imaging of intracellular microviscosity in human breast cancer cells, IJMS **23**(10), 5687 (2022), https://doi.org/10.3390/ijms23105687

[10] I.E. Steinmark, A.L. James, P.-H. Chung, P.E. Morton, M. Parsons, C.A. Dreiss, C.D. Lorenz, G. Yahioglu, and K. Suhling, Targeted fluorescence lifetime probes reveal responsive organelle viscosity and membrane fluidity, PLOS ONE **14**(2), e0211165 (2019), https://doi.org/10.1371/journal.pone.0211165

[11] A.S. Klymchenko, Solvatochromic and fluorogenic dyes as environment-sensitive probes: design and biological applications, Acc. Chem. Res. **50**(2), 366–375 (2017), https://doi.org/10.1021/acs.accounts.6b00517

[12] A. Polita, S. Toliautas, R. Žvirblis, and A. Vyšniauskas, The effect of solvent polarity and macromolecular crowding on the viscosity sensitivity of a molecular rotor BODIPY-C_{10}, Phys. Chem. Chem. Phys. **22**(16), 8296–8303 (2020), https://doi.org/10.1039/C9CP06865A

[13] M.A. Haidekker and E.A. Theodorakis, Molecular rotors–fluorescent biosensors for viscosity and flow, Org. Biomol. Chem. **5**(11), 1669–1678 (2007), https://doi.org/10.1039/B618415D

[14] M.K. Kuimova, Mapping viscosity in cells using molecular rotors, Phys. Chem. Chem. Phys. **14**(37), 12671 (2012), https://doi.org/10.1039/c2cp41674c

[15] A. Vyšniauskas, I. López-Duarte, N. Duchemin, T.-T. Vu, Y. Wu, E.M. Budynina, Y.A. Volkova, E. Peña Cabrera, D.E. Ramírez-Ornelas, and M.K. Kuimova, Exploring viscosity, polarity and temperature sensitivity of BODIPY-based molecular rotors, Phys. Chem. Chem. Phys. **19**(37), 25252–25259 (2017), https://doi.org/10.1039/C7CP03571C

[16] S. Toliautas, J. Dodonova, A. Žvirblis, I. Čiplys, A. Polita, A. Devižis, S. Tumkevičius, J. Šulskus, and A. Vyšniauskas, Enhancing the viscosity-sensitive range of a BODIPY molecular rotor by two orders of magnitude, Eur. J. Chem. **25**(44), 10342–10349 (2019), https://doi.org/10.1002/CHEM.201901315

[17] P. Hohenberg and W. Kohn, Inhomogeneous electron gas, Phys. Rev. **136**(3B), B864 (1964), https://doi.org/10.1103/PhysRev.136.B864

[18] W. Kohn and L.J. Sham, Self-consistent equations including exchange and correlation effects, Phys. Rev. **140**(4A), A1133 (1965), https://doi.org/doi:10.1103/PhysRev.140.A1133

[19] L.W. Chung, W.M.C. Sameera, R. Ramozzi, A.J. Page, M. Hatanaka, G.P. Petrova, T.V. Harris, X. Li, Z. Ke, F. Liu, H.B. Li, L. Ding, and K. Morokuma, The ONIOM method and its applications, Chem. Rev. **115**(12), 5678–5796 (2015), https://doi.org/10.1021/cr5004419

[20] D.A. Case, H.M. Aktulga, K. Belfon, I.Y. Ben-Shalom, S.R. Brozell, D.S. Cerutti, T.E. Cheatham, V.W.D. Cruzeiro, T.A. Darden, R.E. Duke, et al., *Amber 2021* (University of California, San Francisco, 2021).

[21] L. Martínez, R. Andrade, E.G. Birgin, and J.M. Martínez, PACKMOL: A package for building initial configurations for molecular dynamics simulations, J. Comput. Chem. **30**(13), 2157–2164 (2009), https://doi.org/10.1002/jcc.21224

[22] Y. Zhao and D.G. Truhlar, The M06 suite of density functionals for main group thermochemistry, thermochemical kinetics, noncovalent interactions, excited states, and transition elements: two new functionals and systematic testing of four M06-class functionals and 12 other functionals, Theor. Chem. Account. **120**(1–3), 215–241 (2008), https://doi.org/10.1007/s00214-007-0310-x

[23] M.R. Momeni and A. Brown, Why do TD-DFT excitation energies of BODIPY/aza-BODIPY families largely deviate from experiment? Answers from electron correlated and multireference methods, J. Chem. Theory Comput. **11**(6), 2619–2632 (2015), https://doi.org/10.1021/ct500775r

[24] T.H. Dunning, Gaussian basis sets for use in correlated molecular calculations. I. The atoms boron through neon and hydrogen, Chem. Phys. **90**(2), 1007–1023 (1998), https://doi.org/10.1063/1.456153

[25] A.K. Rappé, C.J. Casewit, K.S. Colwell, W.A. Goddard, and W.M. Skiff, UFF, a full periodic table force field for molecular mechanics and molecular dynamics simulations, J. Am. Chem. Soc. **114**(25), 10024–10035 (1992), https://doi.org/10.1021/ja00051a040

[26] V. Barone and M. Cossi, Quantum calculation of molecular energies and energy gradients in

solution by a conductor solvent model, J. Phys. Chem. A **102**(11), 1995–2001 (1998), https://doi.org/10.1021/jp9716997

[27] M.J. Frisch, G.W. Trucks, H.B. Schlegel, G.E. Scuseria, M.A. Robb, J.R. Cheeseman, G. Scalmani, V. Barone, G.A. Petersson, H. Nakatsuji, et al., *Gaussian 16, Revision C.01* (Gaussian Inc., Wallingford CT, 2016).

[28] A. Schlachter, A. Fleury, K. Tanner, A. Soldera, B. Habermeyer, R. Guilard, and P.D. Harvey, The TDDFT excitation energies of the BODIPYs; The DFT and TDDFT challenge continues, Molecules **26**(6), 1780 (2021), https://doi.org/10.3390/molecules26061780

[29] F. Li, S.I. Yang, Y. Ciringh, J. Seth, C.H. Martin, D.L. Singh, D. Kim, R.R. Birge, D.F. Bocian, D. Holten, and J.S. Lindsey, Design, synthesis, and photodynamics of light-harvesting arrays comprised of a porphyrin and one, two, or eight boron-dipyrrin accessory pigments, J. Am. Chem. Soc. **120**(39), 10001–10017 (1998), https://doi.org/10.1021/ja9812047

[30] H. Akima, A new method of interpolation and smooth curve fitting based on local procedures, J. ACM **17**(4), 589–602 (1970), https://doi.org/10.1145/321607.321609

[31] J.J.P. Stewart, Optimization of parameters for semiempirical methods V: Modification of NDDO approximations and application to 70 elements, J. Mol. Model. **13**(12), 1173–1213 (2007), https://doi.org/10.1007/s00894-007-0233-4

[32] A. Prlj, L. Vannay, and C. Corminboeuf, Fluorescence quenching in BODIPY dyes: the role of intramolecular interactions and charge transfer, Helv. Chim. Acta **100**(6), e1700093 (2017), https://doi.org/10.1002/hlca.201700093

BODIPY JUNGINIO NESPINDULINIO BARJERO AUKŠČIO NUSTATYMAS POLINĖJE APLINKOJE TAIKANT ONIOM DAUGIASLUOKSNĮ METODĄ

D. Narkevičius, S. Toliautas

Vilniaus universiteto Fizikos fakultetas, Vilnius, Lietuva

Santrauka

Fluorescuojantys molekuliniai jutikliai yra plačiai naudojami biologiniuose tyrimuose. Jie leidžia nesudėtingai pamatuoti klampą, temperatūrą ar poliškumą mikroskopiniu lygmeniu, įskaitant gyvas ląsteles. Ląstelėms taikant fluorescencijos gyvavimo spektroskopiją (FLIM) galima gauti norimų fizikinių savybių žemėlapius.

Viena svarbiausių ląstelės savybių yra klampa, nes ji turi įtakos kitiems parametrams, pvz., biocheminių reakcijų greičiui ir dalelių difuzijai. Boro-dipirometeno (BODIPY) junginiai yra plačiai naudojami matuojant klampą, tačiau dabartiniai variantai turi nepageidaujamą jautrumą poliškumui, todėl tinkamesnių alternatyvų ieškoma taikant kompiuterinius skaičiavimus. Ankstesniuose tyrimuose naudotas poliarizuoto kontinuumo modelis (PCM) netinkamai įvertino polinės aplinkos įtaką skaičiuojant aktyvacijos energiją, siejamą su jautrumu poliškumui.

Taikant daugiasluoksnį ONIOM metodą polinėje bei nepolinėje aplinkose buvo apskaičiuoti 8-Ph-BODIPY junginio fluorescencijos spektrų maksimumų bangos ilgiai, kurie geriau atitiko eksperimentinius rezultatus palyginti su PCM. Taip pat buvo apskaičiuota aktyvacijos energija, kurios vertė polinėje ir nepolinėje aplinkoje kokybiškai atitiko eksperimentinius rezultatus, o taikant empirinę korekciją – ir kiekybiškai.